Beamforming for Millimetre-wave NOMA

Cian Dowd

The thesis is submitted to University College Dublin
in part fulfillment of the requirements for the degree of

Master of Engineering

College of Engineering and Architecture
School of Electrical & Electronic Engineering

Head of School: Prof. Peter Kennedy
Supervisor: Le-Name Tran

July 2019

For family and friends, with love.

Acknowledgements

First, I would like to thank my family, especially my parents, for all of their support. Without you, none of this would have been possible. You have been incredibly generous, and more understanding than was fair to expect. The help and care you unconditionally offer are what has gotten me this far.

I also want to thank my friends. You were very encouraging and helped to keep me positive throughout. Thank you for all you have done, big and small. You made this whole process more manageable, but you have also made it enjoyable.

Finally, I would like to express my appreciation to Dr. Le-Nam Tran for his supervision and guidance throughout this thesis. Throughout you have been very generous with your time and very thoughtful in your critiques of this research.

Abstract

Non-Orthongonal Multiple Access (NOMA) will be an important technology in enabling Future Radio Access (FRA) and the next generation of wireless networks. NOMA shares orthogonal resources amongst connected devices to improve spectral efficiency. This is done through power domain multiplexing within those resources.

This thesis will examine the success of NOMA when interfacing beamforming (BF) and Millimetre-wave (mmWave) spectrum, which are both to be facets of 5G networks as well.

A review of the literature pertaining to NOMA and related technologies is conducted. Challenges facing NOMA, such as receiver complexity and Path Loss Ratio (PLR) are outlined and later tackled.

A realistic mmWave channel model is chosen as the basis for all simulations of NOMA systems. This benefits the work as it puts it in the correct frame of reference.

The performance of Zero Forcing (ZF) and Maximum Ratio Transmission (MRT) BF algorithms are analysed and MRT is chosen as the more successful approach for NOMA.

Different schemes are considered and optimal Power Allocation (PA) is achieved with significantly reduced processing. Hybrid NOMA (H-NOMA) with Proportional Fairness (PF) is found to be a scheme which realises the best sumrates, other than full NOMA, while reducing the complexity and overhead of full NOMA.

Lay-Abstract

This thesis explores Non-Orthongonal Multiple Access (NOMA) and how it can be used with beamforming (BF) and Millimetre-wave (mmWave) frequencies.

Cellular networks communicate with devices through radio waves, which includes mmWave frequencies. BF is a way for cell towers to steer signals towards those devices.

Traditionally, cell towers may have communicated with one device at a time, or using a single resource per device. NOMA allows multiple devices to share those same resources. This is important due to the finite nature of those resources.

This thesis proposes multiple methods of combining these technologies in future mobile networks and finds that not only is it feasible but that sharing resources, as NOMA aims to, is beneficial.

Contents

List of Tables

List of Figures

List of Acronyms

ADC analogue-to-ditial convertor

BF beamforming

BF-NOMA NOMA within Beamforming Beams

BFS Brute Force Search

BS Base Station

CCU Cell Centre User

CDMA Code Division Multiple Access

CEU Cell Edge User

CSI Channel State Information

FDMA Frequency Division Multiple Access

FOA First Order Approximation

FRA Future Radio Access

H-NOMA Hybrid NOMA

LOS Line of Sight

MA Multiple Access

mmWave Millimetre-wave

MRT Maximum Ratio Transmission

NLOS Non-Line of Sight

NOMA Non-Orthongonal Multiple Access

OFDMA Orthongonal Frequency Division Multiple Access

OMA Orthongonal Multiple Access

PA Power Allocation

PF Proportional Fairness

PL Path Loss

PLE Path Loss Exponent

PLR Path Loss Ratio

RAN Radio Access Networks

SIC Successive Interference Cancellation

SINR Signal to Interference and Noise Ratio

TDMA Time Division Multiple Access

UE User Equipment

UPPA User Pairing and Power Allocation

ZF Zero Forcing

Chapter 1

Introduction

NOMA is an important Multiple Access (MA) technology for the future of wireless networks and has great potential for 5G. With a trend towards mmWave, MIMO, and BF it is important to consider the strengths and weaknesses of these technologies together and how they can be used in future radio networks.

NOMA is different from conventional Orthongonal Multiple Access (OMA) technologies by allowing more than one User Equipment (UE) to access shared resources at a time. This is ever more important as demands for connectivity rise and increase the importance of spectral efficiency in our communications.

The challenges faced by NOMA will be discussed and potential solutions will be evaluated. Analysis will be done through the lens of mmWave spectrum and with the aim of maximising the sumrates of systems, which use NOMA for MA and have a Base Station (BS) which can use BF.

mmWave spectrum will bring greater bandwidths and has the potential for much higher capacity. However, it brings its own set of limitations as well. Higher frequencies will attenuate signals further and mmWave will have further challenges still as it is less likely to refract around, or penetrate through, obstacles as other Radio Frequency signals do..

This thesis will consider these challenges and propose solutions through various NOMA schemes and means of implementing NOMA which reduce adverse effects. First, a review of the current literature on these topics is conducted. Then, the technologies are tested by series of simulations, comparing and contrasting various aspects of NOMA systems.

Chapter 2

Background/ Literature Review

In this chapter we will explore existing MA techniques, basic NOMA systems, and research to date within the field of NOMA.

2.1 Existing Multiple Access Technologies

MA techniques allows multiple devices to share a medium in communications. These techniques improve the efficiency of communicating over a medium and are relevant to mobile communications networks, as they use finite media to communicate wirelessly with mobile UEs.

MA techniques used, in mobile networks to date, include:

1G Frequency Division Multiple Access (FDMA)

2G Time Division Multiple Access (TDMA)

3G Code Division Multiple Access (CDMA)

4G Orthongonal Frequency Division Multiple Access (OFDMA)

This is due to the constant growth in mobile use and data use in particular.

While FDMA and TDMA allow users to use one frequency or time resource, respectively, newer MA allows improved sharing of resources. CDMA allowed multiple UEs to use the same frequencies simultaneously, separating signals with orthogonal codes. OFDMA or OMA uses orthogonal frequencies to allow more UEs to communicate contemporaneously within a tighter grouping of frequencies.

Though CDMA and OFDMA have improved spectral efficiency compared to FDMA andTDMA sharing orthogonal resources, as in NOMA, increases the spectral efficiency of the system further still. Consider the throughput of a Cell Edge User (CEU) in an OMA system. In OMA the CEU claims the whole resource but the throughput of the device is low due to channel conditions at the cell edge. Under NOMA, CEU can share those resources with Cell Centre User (CCU) that have better channel conditions, and therefore more efficient use of the spectrum.

2.2 Basic NOMA

Power-Domain NOMA can serve multiple users in the same orthogonal resource (time slot, orthogonal code, or orthogonal frequency) by using power multiplexing to perform multiple access. This is done by allocating different powers to different users. [1] Assigning different power levels to individual users allows each user to decode their signal using Interference Cancellation techniques.

Figure 2.1 shows a simple two-user and BS NOMA downlink system. The following description of a Basic NOMA system follows [1–3]. Taking UE_1 as a CCU and UE_2 as the CEU, we can say that their distances d_i from the BS fit $d_1 \leq d_2$. For the same carrier frequency, we can then say that the channel gains, $|h_i|^2$, at the UE's fit $|h_1|^2 \geq |h_2|^2$. The powers, P_i, can then be described by $P_1 \leq P_2$, where $P_1 + P_2 = P_{total}$. The signals sent to the UE's are superposed atop each other, summing to the maximum power of the system.

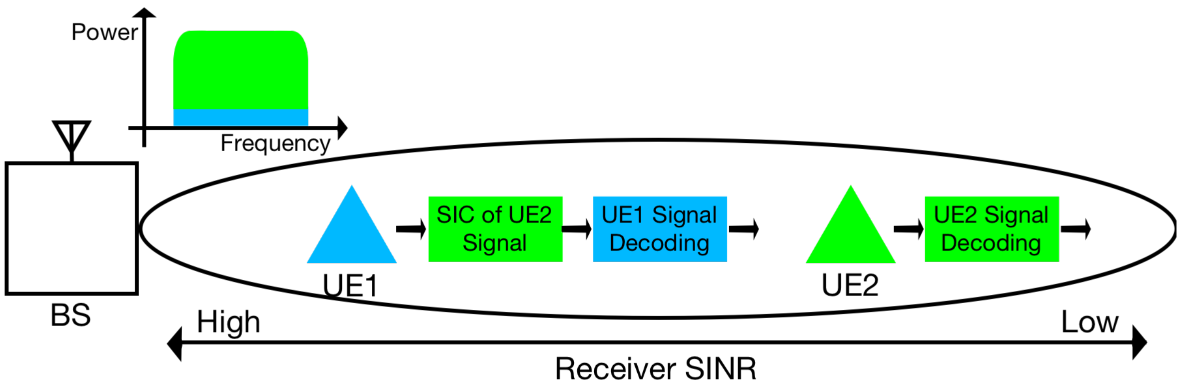

Figure 2.1: Basic NOMA with SIC for Two UE Receivers in Downlink

To decode the signals, in downlink NOMA, Successive Interference Cancellation (SIC) is used. For N users with channel gains $|h_i|^2$ if $|h_1|^2 \geq |h_2|^2 \geq \ldots \geq |h_N|^2$ then each user applies SIC to $N - i$ signals before decoding their own. In the two user case that means that UE_2 only decodes their own message, treating UE_1's message as noise, while UE_1 performs SIC then decodes its message.

The achievable rate is given generally by equation (2.1):

$$R_i = \log_2 \left(1 + \frac{P_i \cdot |h_i|^2}{\sum_{n=1}^{i-1} P_n \cdot |h_i|^2 + N_0} \right) \tag{2.1}$$

In the specific case of a 2-UE NOMA system the rates of UE_1 and UE_2 are given by equation (2.2) and equation (2.3) respectively:

$$R_1 = \log_2\left(1 + \frac{P_1 \cdot |h_1|^2}{N_0}\right) \tag{2.2}$$

$$R_2 = \log_2\left(1 + \frac{P_2 \cdot |h_2|^2}{P_1 \cdot |h_2|^2 + N_0}\right) \tag{2.3}$$

As was discussed above, equation (2.2) shows that UE_1 suffers no interference from UE_2. Though UE_1 is assigned less power, which hinders its rate, being able to remove the interfering signal boosts its rate. The converse is true for UE_2 which is assigned more power but has its rate hindered by the interfering signal of UE_1, shown in equation (2.3).

2.3 Beamforming Algorithms

BF is a process by which devices with multiple antennas can control the direction of their transmission. A transmission using BF has two components:

- Power Allocation
- Direction

Direction is given by what is called a BF precoder. The purpose of a BF algorithm is to determine a precoder for a UE. This section will consider two popular BF algorithms.

2.3.1 Zero Forcing Beamforming

This subsection follows details of ZF BF outlined in [4, 5]. The primary aim of ZF BF is to nullify inter-UE interference by forcing the power transmitted in the direction of other UEs to zero, hence the name. ZF focuses on the nullification of interference over maximising power in the direction of the target UE. Direction of a UE is determined by the channel, assumed through Channel State Information (CSI).

The nulling property of ZF BF is what makes it of interest for NOMA systems. As CEUs must endure inter-UE interference, as they do not perform SIC, ZF may reduce the interference they experience, increase their throughput, and by extension increase the sumrate of the system. This increase in CEU throughputs may be sufficient to overcome the fact that ZF BF does not maximise power in the direction of the target UE.

ZF may cause issues for NOMA as the inter-UE interference is what CCUs use to do SIC and later reduce their interference. The effects of this may be seen in the results of future simulations.

Equation (3.13) shows the ZF algorithm used to generate the precoder.

2.3.2 Maximum Ratio Transmission

This subsection follows details of MRT BF outlined in [6, 7]. MRT contrasts with ZF as this algorithm prioritises the maximisation of each individual UE's throughput over all else. By prioritising the throughput of the target UE, other UEs may experience some degree of interference by neglecting to consider their presence.

MRT assumes that the benefits of maximising transmission power outweigh the cons. In a NOMA system this means that sumrate may increase as the signal strength of each UE is maximised. The sumrate of each UE is also impacted, however, by all other UEs having their signal strength maximised.

As MRT does cause inter-UE interference there should be no hindrances to the SIC process. This leaves MRT indifferent when considering CCUs but may make it a worse option for CEUs.

Equation (3.15) shows the MRT algorithm used to generate the precoder.

2.4 Optimising NOMA

There have been many investigations into how to improve upon basic NOMA techniques. In this section we will explore some of these improvements.

2.4.1 Hybrid NOMA

H-NOMA is the concept of creating a NOMA system within an orthogonal resource of another OMA system. For example, within an OFDMA resource two UEs could share the orthogonal frequency and treat it as a single NOMA resource [1]. This is useful as to serve all UEs in a cell on a single NOMA resource would not be feasible.

The idea is highly dependant on User Pairing and Power Allocation (UPPA) as a greater PLR will increase the rates achievable by all UEs involved [8]. H-NOMA has appeal in the literature as existing OMA techniques are mature and well understood. The blending of traditional techniques with a means of improving spectral efficiency is very appealing.

It is noteworthy that a CCU may achieve a better rate with NOMA than with traditional OMA while a CEU is likely to achieve a worse rate with NOMA than OMA [1].

2.4.2 Grouping UEs

Related to H-NOMA, but also an area of interest in basic NOMA too, is the pairing of UEs in NOMA systems. UPPA is crucial to the success of NOMA which has lead to many investigations into H-NOMA and PA algorithms.

One such investigation was into a Tree-search based Transmission Power Assignment [9]. This is particularly novel for it is an ideal solution without conducting an exhaustive search.

2.4.3 mmWave NOMA

The use of mmWave spectrum as a carrier for NOMA and beamforming is well known. Limited spectrum in our current frequency bands makes mmWave spectrum the obvious home for future growth.

It has been noted that mmWave frequencies are well aligned for both beamforming and NOMA as they both benefit from MIMO [1]. This is as a result of mmWave allowing for smaller antennas, which in turn allow for tighter antenna arrays. MIMO is of course essential for beamforming and benefits NOMA as strong channel vector correlation is beneficial to both MIMO and NOMA.

2.5 Limitations & Challenges

The following section addresses some of the main limitations and future challenges against NOMA. These are areas which may require research and are potential directions for this project to work.

2.5.1 Path Loss Ratio

NOMA can may only be applied when the PLR between UE's is roughly 8 dB or higher and the rates of NOMA users improves with greater PLRs [8, 10, 11]. This poses as a limitation in how users can be paired in NOMA and how power can be allocated at the BS.

Due to the critical importance of PA and PLRs to the success of NOMA coming up with effective PA algorithms is of the utmost importance. Similarly, for H-NOMA, UPPA is of great importance as there is the potential to split UEs into different OMA resources as well as performing PA.

2.5.2 Receiver Complexity

The SIC aspect to NOMA introduces a lot of complexity to the receivers [11, 12]. The SIC order, needs to be communicated to the receivers. SIC needs to be carried out correctly or errors will propagate and require retransmission, lowering the throughput of the system. There is also additional overhead simply in the decoding of the signal. All of these factors may hinder make the receivers harder to design and more energy demanding to run.

2.5.3 Quantisation Error

Quantisation error in the analogue-to-ditial convertor (ADC) may cause errors for the receiving UE during the signal processing [12]. As some signals will be very weak, particularly compared to the large signals that are to be removed by SIC, the ADCs must support a large input range with a very high resolution. High resolution ADCs can be cost prohibitive and but a certain threshold must be met to support NOMA. A trade off will have to be made between quantisation error and the performance of SIC in these NOMA receivers.

Chapter 3

Methods and Results

To understand NOMA and to create a test-bed to compare future work against I ran simulations of NOMA in MATLAB.

3.1 Finding a Suitable Channel Model

As a focus of the project is the performance of NOMA in mmWave spectrum I first did work to find a suitable mmWave Channel model. Finding such a channel model is important as it has a direct effect on the rate's each NOMA user can achieve. Throughput, or some derived metric, will be used to determine the success of different PA schemes and for comparing PA schemes to each other.

3.1.1 Friis' Transmission Equation

It was assumed that a conventional channel model, similar to those used for modern mobile networks, would be unrealistic in it's optimism as the higher frequencies of mmWaves will weaken faster. To show this Friis' Transmission Equation for Path Loss (PL), equation (3.1), was taken as a control for comparing other channel models. A weakness of Friis' Equation is that it assumes free space propagation. Some channel models use Friis' as a base with some additional loss to account for Non-Line of Sight (NLOS) propagation [13].

$$20 \cdot \log_{10}\left(\frac{4\pi df}{c}\right) \tag{3.1}$$

Where:

d is the distance between UE and BS

f is the frequency of the carrier

c is the speed of light

3.1.2 Path Loss Exponent

A common adaptation of the Friis' Equation is the PLE Equation, shown in equation (3.2). PLE is a common adaptation as the variable exponent is used to counteract the free space Line of Sight (LOS) assumption of Friis' Equation.

$$10\beta \cdot \log_{10}\left(\frac{4\pi df}{c}\right) \tag{3.2}$$

Where β is the exponent and other variables are as above.

I chose to use an exponent value of 3.4 as it is commonly used for 28 GHz NLOS channel models [14–16]. Using figures tuned for NLOS is sensible as it allows for more realistic simulations. LOS is very rare in mobile communications, particularly in urban spaces, where mmWave is likely to be deployed fist. I believe that 28 GHz spectrum is a realistic estimate for frequency also. Though 28 GHz is within mmWave spectrum it will be easier to produce hardware for that higher frequencies and it will propagate further than higher frequencies, allowing fewer BSs to provide coverage.

3.1.3 NYU Empirical Model

[17] shows an empirical model for mmWave, based on results from New York City. This model describes large scale fading by equation (3.3).

$$PL(d)[\mathrm{dB}] = \alpha + 10\beta \cdot \log_{10}(d) \tag{3.3}$$

Once more, choosing values for an NLOS 28 GHz channel model we get $\alpha = 72.0$ and $\beta = 2.92$. The justifications for these conditions seen above.

3.1.4 Comparing Models

Figure 3.1 shows a comparison of the PL that the above channel models discuss. The carrier frequency is assumed to be 28 GHz, where applicable values assume NLOS, and the distances are 88 m and 330 m for the CCU and CEU respectively.

One can see that free space propagation, modelled by equation (3.1) and graphed as PL, is by far the most optimistic of the models. This is to be expected due to the

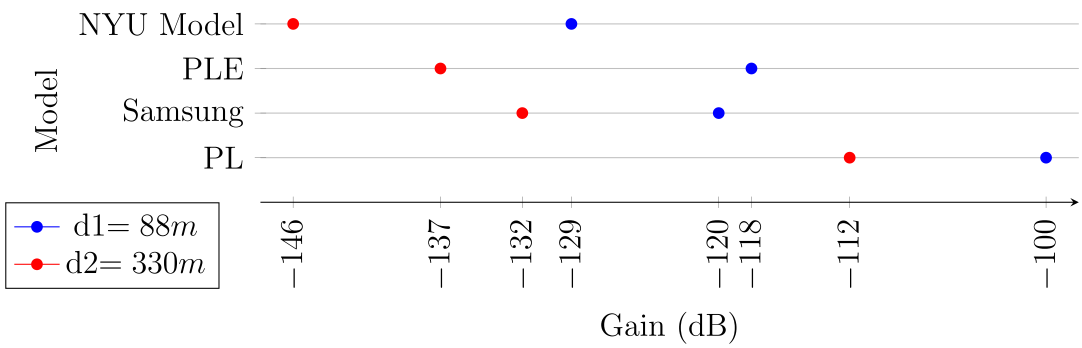

Figure 3.1: Graph Comparing the PL Calculated by Various Channel Models

simplifying assumptions it makes.

Samsung's model [13], free space propagation with an additional 20 dB loss, is comparable to PLE for the CCU but is more optimistic than PLE for the CEU. It is interesting to note that an additional 20 dB loss is still quite optimistic as compared to more complex models.

We can see that the model shown in equation (3.3), with the values described above, is more pessimistic than the other models. It aligns with results found in [17], which say measured results were about 30 dB weaker than free space propagation. Comparing the results of equation (3.3) to equation (3.2) the relative loss of the CCUs is greater than that of the CEUs.

I believe that the NYU model, detailed above, is a suitable model to use for the large scale fading going forward. It is clear that Friis' Equation, and Samsung's adaption, are far too optimistic. Though I believe that the values selected for PLE are well founded in the literature, I believe that the empirical model proposed by NYU will give harsher testing. Harsher models can be seen as a worst case scenario and useful for testing the feasibility of NOMA and results of tests and simulations.

3.2 Basic NOMA Simulations

With the channel model chosen, per section 3.1, rate simulations of NOMA systems were conducted using equation (2.1) to calculate the rate. In these simulations the conditions were as follows:

3.2.1 Channel Model

The large scale fading of the channel model is as described in section 3.1, this equates to the PL of the signal and is largely dependent on distance and frequency. To finalise the channel model small-scale fading was represented by summing random complex numbers to the PL figure. The small-scale fading has not much effect on the basic NOMA case, as there is only one antenna on each UE and the BS, though it adds some variation to independent simulations.

3.2.2 Distances

In each simulation distances for each of the UEs are randomly generated, independent of each other, but were ultimately sorted by least to greatest. The distances of the different UEs fell within the range of 50 m to 250 m. These distances were chosen to reflect a CCU and a UE at the likely edge of a mmWave small cell network [18].

3.2.3 Power Allocation

The PA for these early simulations was to run brute force calculations for each UE. This is to say that, particularly with a 2-UE simulation the powers assigned can all be known and can all be computed. This is not efficient but given the low degree of complexity inherent in these systems it is sufficient.

3.2.4 2-UE Simulations

Figure 3.2 is representative of the results found from basic NOMA simulations, following the conditions outlined above.

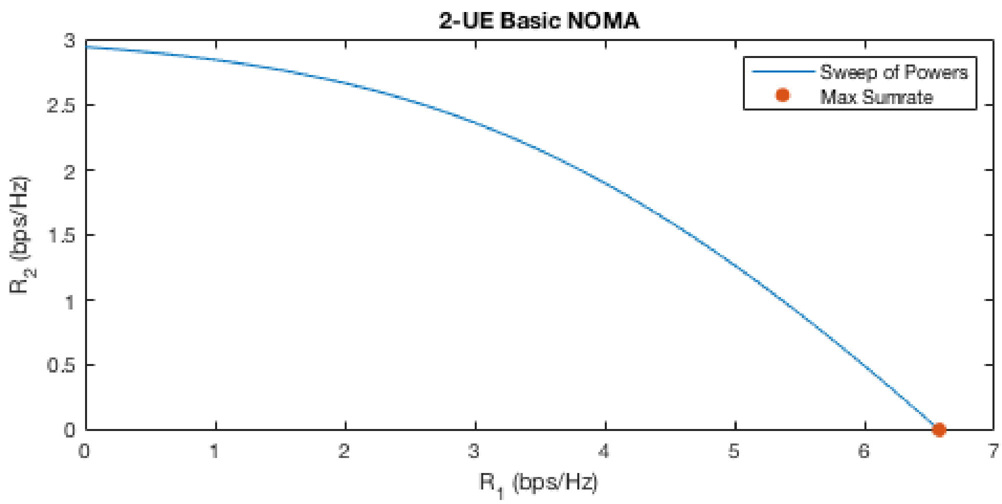

Figure 3.2: 2-UE NOMA Rate

It is clear to see that these simulations greatly favour the CCU. The rates achieved by the CEU are low and the best sumrates are achieved by excluding that UE. These results are quite pessimistic and are not promising for the promise of NOMA generally.

The results seen in figure 3.2 are indicative of UE_1 benefiting from good SIC while UE_2 suffering from interference. It is clear, therefore, that more successful results would require better PA to the CEU for the relative ratio of distances. Alternatively, if the

CEU were closer to the cell centre losses across the channel would be lowered, perhaps improving throughput.

3.3 Beamforming NOMA

The conditions and assumptions for the BF simulations were similar to those in section 3.2.

In the basic NOMA simulations, small-scale fading added variability to the only channel between BS and UE. The key difference for these simulations is that there are more antennas at the BS. This has two main effects:

- The small-scale fading in the channel model now introduces variability for all channels between BS antennas and a UE.
- The throughput calculation now computes, for each set of powers, the throughput at different beamforming nodes. This is equivalent to considering non-uniform radiation patterns that can be seen with beamforming techniques.

The addition of extra BS antennas has the opportunity to increase the throughput of individual UEs and, by extension, the sumrate of the system. Using many antennas allows transmissions to take on a directionality, as compared to isotropic transmission, though radiation patterns will still be imperfect. This allows for more efficient use of power, increasing the power of the signal at a receiving UE. Another benefit of directionality, aside from increasing the power at the desired receiver, is the potential reduction in inter-UE interference. Reducing interference would benefit other UEs and as a result benefits the system throughput as a whole. The benefits of beamforming, of course, being derived from the relationship between Signal to Interference and Noise Ratio (SINR) and throughput.

3.3.1 System Model

Notation and Equations

The system comprises of a BS, with 16 antennas (N_{Tx}), and 2–8 UEs (K), the number of UEs stated when relevant. The BS uses NOMA and BF to communicate with the UEs. The aim is to optimise the Power Allocation while using a BF algorithm to get the direction of the beam.

The channel model is, as discussed above in sections 3.1 and 3.2.1, based on PL, given by equation (3.3), and small scale fading, which also implies a directionality. Let $\mathbf{h}_k \in \mathbb{C}^{N_{\mathrm{Tx}} \times 1}$ be the channel for UE k. Similarly, let $\mathbf{w}_k \in \mathbb{C}^{1 \times N_{\mathrm{Tx}}}$ be the beamformer for UE k which is given by

$$\mathbf{w}_k = \sqrt{\beta_k}\mathbf{u}_k \tag{3.4}$$

Where β_k is the PA for UE k and $\mathbf{u}_k \in \mathbb{C}^{1 \times N_{\mathrm{Tx}}}$ is the BF direction, or the BF precoder, for UE k. This will be determined by the BF algorithm employed.

The received signal at UE k is

$$y_k = \sum_{j=1}^{k-1} \mathbf{w}_j \mathbf{h}_k + \mathbf{w}_k \mathbf{h}_k + \sum_{j=k+1}^{K} \mathbf{w}_j \mathbf{h}_k + n_k \tag{3.5}$$

Suppose that SIC is performed from UE K to UE $k+1$. The interference caused by UEs from $k+1$ is removed. Thus, the SINR at UE k is given by

$$\gamma_k = \frac{\left|\mathbf{w}_k \mathbf{h}_k\right|^2}{\sum_{j=1}^{k-1} \left|\mathbf{w}_j \mathbf{h}_k\right|^2 + N_0} = \frac{\left|\sqrt{\beta}_k \mathbf{u}_k \mathbf{h}_k\right|^2}{\sum_{j=1}^{k-1} \left|\sqrt{\beta}_j \mathbf{u}_j \mathbf{h}_k\right|^2 + N_0} \tag{3.6}$$

$$= \frac{\beta_k \left|\mathbf{u}_k \mathbf{h}_k\right|^2}{\sum_{j=1}^{k-1} \beta_j \left|\mathbf{u}_j \mathbf{h}_k\right|^2 + N_0} \tag{3.7}$$

The achievable rate of UE k is given by

$$R_k(\boldsymbol{\beta}) = \log(1+\gamma_k) \tag{3.8}$$

$$= \log\left(1 + \frac{\beta_k \left|\mathbf{u}_k \mathbf{h}_k\right|^2}{\sum_{j=1}^{k-1} \beta_j \left|\mathbf{u}_j \mathbf{h}_k\right|^2 + N_0}\right) \tag{3.9}$$

$$= \log\left(\beta_k \left|\mathbf{u}_k \mathbf{h}_k\right|^2 + \sum_{j=1}^{k-1} \beta_j \left|\mathbf{u}_j \mathbf{h}_k\right|^2 + N_0\right) - \log\left(\sum_{j=1}^{k-1} \beta_j \left|\mathbf{u}_j \mathbf{h}_k\right|^2 + N_0\right) \tag{3.10}$$

Simulation Parameters

The distances that are used as the variable inputs to equation (3.3) are randomly generated within the range of 50 m to 250 m. This follows the reasoning given in section 3.2.2. Keeping these conditions consistent allows for a more direct comparison between NOMA with BF versus Basic NOMA.

Before a transmission to the connected UEs the BS ranks the UEs based on the norm of their effective channels, the norm of the 16 channel values. Sorting UEs based on this norm sorts them from strongest to weakest, similar to CCU–CEU, allowing for SIC in a NOMA system. Ranking UEs like this is particularly important for scheduling in H-NOMA and BF-NOMA schemes but simply used for SIC order otherwise.

The problem of BF for a NOMA system can be decomposed into two parts:

- Creating beams to target UEs
- UPPA or Scheduling and PA

These problems were approached independently, first testing the effectiveness of BF in NOMA systems before choosing a suitable BF algorithm, and then finding a suitable means of UPPA.

3.3.2 Random Beamforming

Random BF was used to test the viability of BF in this system. Though it can be intensive to simulate a large set of random beams it can be indicative of an optimal result. Therefore, comparing the resilts of random BF with the brute force seach results from the basic NOMA system in section 3.2

At this point PA is still done by a Brute Force Search (BFS). Given that, and adding the complexity of using a brute force process to create random beams, it is only practicable to perform tests for systems with 2 or 3 UEs. This shall be sufficient for the purpose of comparing to results from section 3.2, as similar constraints limited the number of UEs there also.

Equation (3.11) defines the random BF precoder:

$$\mathbf{u} = \mathrm{rand}(1, N_{\mathrm{Tx}}) \tag{3.11}$$

Where $\mathrm{rand}(x, y)$ creates a vector of random numbers with x rows and y columns. Consequently, the beamformer for UE k is given by

$$\mathbf{w}_k = \sqrt{\beta_k}\ \mathrm{rand}(1, N_{\mathrm{Tx}}) \tag{3.12}$$

A random vector is used here, in place of a traditional BF algorithm, to test the feasibility of BF generally.

2-UE Simulations

Simulations of 2-UE NOMA systems, with systems characterised as above, yielded the following results.

Figure 3.3 is representative of the most promising results of these 2-UE BF simulations.

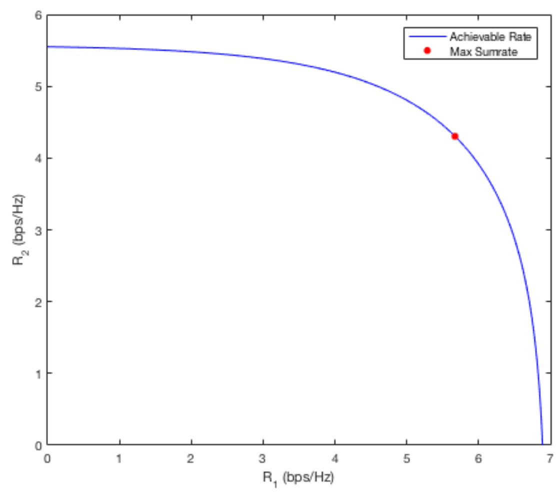

Figure 3.3: 2-UE BF NOMA Rate

It is clear to see from figure 3.3 that the maximum sumrate of system is a rate which is non-exclusionary, unlike the results seen in section 3.2.4. Achieving maximum sumrate in the middle of the curve of achievable sumrates is noteworthy as it shows that NOMA has the potential to improve spectral efficiency in absolute metrics. This is to say that, in this simulation, NOMA achieved a better rate by sharing the available spectrum than would have been possible if the spectrum were used by only one UE. Contrasting figure 3.3 with figure 3.2 we can see that BF made a noticeable improvement to the rate of the whole system, though a greater improvement to the rates seen by CEUs.

3-NOMA Simulations

For the 3-UE BF NOMA simulations the conditions were the same as the 2-UE equivalents. A key difference with the 3-UE case is that the PA problem gets much more complicated, complexity grows with UEs.

For some 3-UE simulations the maximum rate was such that all three UEs had a respectable rate. Figure 3.4 shows one such example.

In the simulations ran the results in figure 3.4 were quite common. However, another common result is that akin to what can be seen in figure 3.5, where one UE would be excluded.

It is clearly ideal to have rates which permit more UEs, this is to say results more like those in figure 3.4 than in figure 3.5. From examining the circumstances leading to these separate results it is clear that PLR is the key factor in how successful all three UEs will be. Where in Basic NOMA it may be preferable to choose two UEs with the greatest difference in channels [8], this random BF technique tended to favour UEs with similar PL, to a point. If two UEs were within $\sim$1 dB then typically the two UEs with the greatest PL difference achieved the best rate, as was the case in figure 3.5.

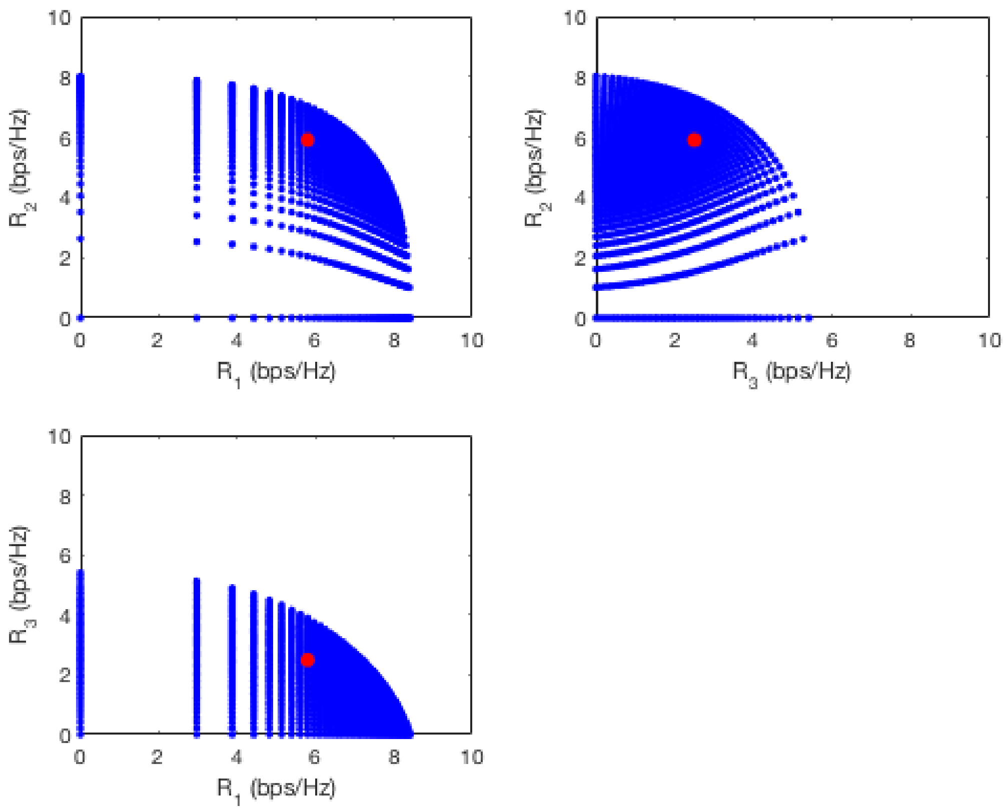

Figure 3.4: 3-UE BF NOMA Rate — Including All

3.3.3 Beamforming Algorithms

Given the success of random BF seen in section 3.3.2 we can see that there are measurable benefits to using BF with NOMA. However, random BF is not feasible in real systems as it is too resource intensive. This leads us to consider some common BF algorithms to generate the precoder, or to determine the direction of the beam.

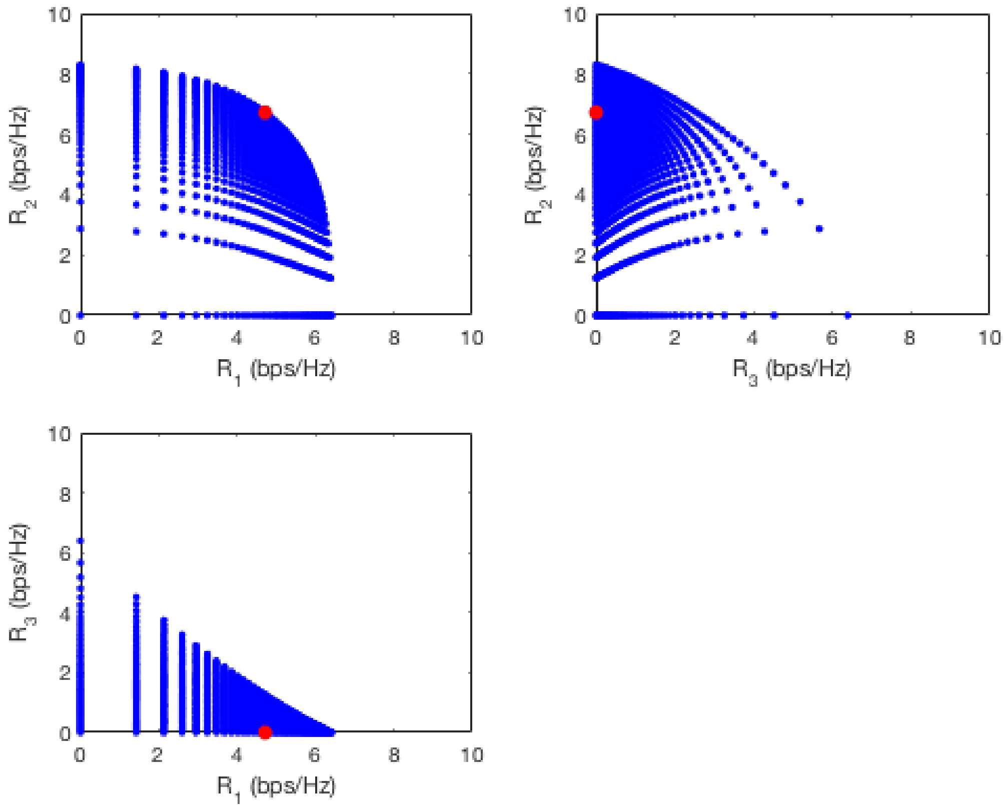

Figure 3.5: 3-UE BF NOMA Rate — Including UE_1 and UE_2

Zero Forcing Beamforming

ZF is a BF algorithm which aims to create nulls in the direction of other UEs, hence the name Zero Forcing. ZF gives priority to reducing inter-UE interference over maximising power in the direction of the desired UE. While this lowers the throughput of any one UE, ZF BF can be beneficial to the sumrate of the system as reduced interference boosts the throughput of other UEs.

Equation (3.13) defines the BF precoder for ZF as:

$$\mathbf{u} = \frac{\mathbf{H}^{\dagger}}{||\mathbf{H}||_2} \tag{3.13}$$

Where $(\cdot)^{\dagger}$ denotes the pseudo-inverse operation, which is defined as $\mathbf{H}'(\mathbf{H}\mathbf{H}')^{-1}$, and $||\cdot||_2$ denotes the ℓ_2-norm. Consequently, the beamformer for UE k is given by

$$\mathbf{w}_k = \sqrt{\beta_k}\frac{\mathbf{H}^{\dagger}}{||\mathbf{H}||_2} \tag{3.14}$$

The pseudo-inverse operation, used in ZF, serves to create beams which create nulls in the directions of non-intended recipients of the signal.

Maximum Ratio Transmission Beamforming

MRT is a BF algorithm which prioritises the maximisation of power in the direction of the desired UE over the other factors, such as reducing inter-UE interference. This maximises the transmission power in the direction of the UE, giving each UE the best signal strength possible.

The BF precoder for MRT is given by equation (3.15):

$$\mathbf{u_k} = \frac{\mathbf{h_k}^H}{||\mathbf{h_k}||_2} \tag{3.15}$$

Where $(\cdot)^H$ denotes the Hermitian operation and $||\cdot||_2$ denotes the ℓ_2-norm. Consequently, the beamformer for UE k is given by

$$\mathbf{w}_k = \sqrt{\beta_k}\frac{\mathbf{h}_k^H}{||\mathbf{h}_k||_2} \tag{3.16}$$

The Hermitian transpose, used in MRT, serves to direct the beam in the direction of the UE, as determined by CSI.

ZF vs MRT

Simulations of both ZF and MRT were run, with NOMA as the means of MA, to determine the best BF algorithm to use in a NOMA system. One may expect ZF to have superior performance due to the reduction of inter-UE interference, or for MRT to achieve better sumrates as SIC may be sufficient and higher signal strength may be a more important factor. The simulations were necessary as it is not obvious which factors would lead to better system throughput overall.

The maximum sumrates achieved using both ZF and MRT are shown in table 3.1. The numbers in this table pertain to the rate graph in figure 3.6:

Table 3.1: ZF and MRT Max Sumrates

BF Method	Sum Rate (bps/Hz)
MRT	7.0
ZF	7.0

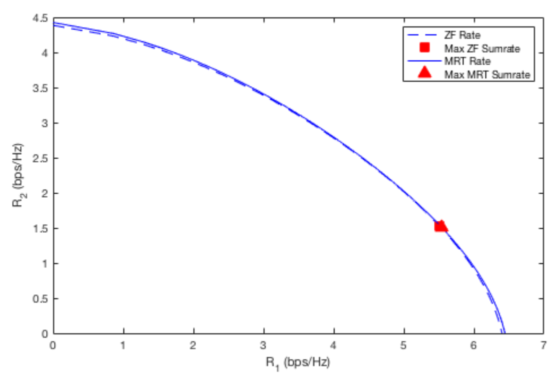

Figure 3.6: 2-UE NOMA ZF BF vs MRT BF

In figure 3.6 it is clear that the two BF algorithms have comparable performance in this system on average. However, it can be seen in the figure that MRT is superior, by a slim margin, to ZF at all points along the sumrate curve. Results in table 3.1 don't quite reflect this as the results were closest at the optimal point on this curve and the precision is insufficient to show that here.

Though the results were comparable, as MRT achieved the best sumrates it is the BF algorithm that will be used going forwards. Therefore, the beamformmer from equation (3.16) is adopted as the beamformer for the rest of this thesis.

3.3.4 User Pairing and Power Allocation for Beamforming NOMA

Based on research presented above detailing NOMA schemes and UPPA for NOMA, the following schemes were considered as solutions to this aspect of BF for NOMA.

- Brute Force Search
- An Iterative Algorithm
- H-NOMA
- H-NOMA with PF
- NOMA within BF Beams

Brute Force Search

A BFS is a very effective but inefficient way of finding the optimal PA for a given system at a given time. All possible PA combinations are computed to find the solution which yields the greatest sumrate. Equation (3.9) equation is computed for each UE for each set of PAs and then the rates are summed.

Results from simulations of the BFS approach can be seen in figure 3.7

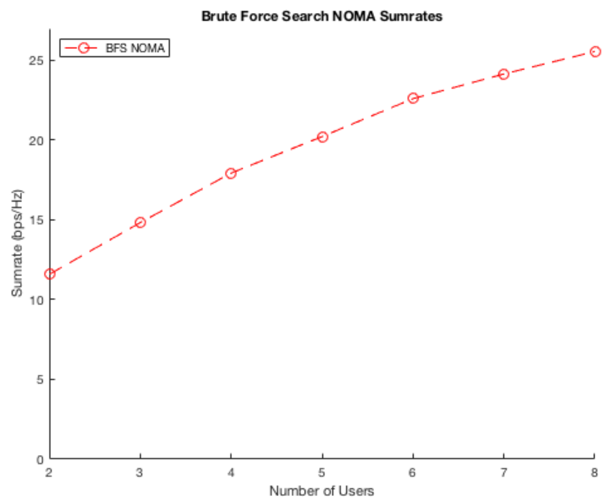

Figure 3.7: BFS NOMA Results

It can be seen that adding more UEs to the NOMA system increases the sumrate for K 2 to 8. It is noticeable that the rate does not increase steadily. Instead there are diminishing increases to sumrate for each additional UE. This is sensible as each UE may put additional strain on the SINR of other UEs and may not add much to the system throughput.

Iterative Algorithm

Though BFS will find the optimal PA for a given K-UE systems, BFS for PA becomes too resource intensive to be practical when K is relatively large. An iterative algorithm may serve as a more efficient and equally effective solution to finding the best PA for a set of UEs. As the sumrate of a NOMA system may be non-convex, the iterative algorithm will instead optimise a First Order Approximation (FOA) of the equation for sumrate.

Equation (3.17) is a FOA expansion of equation (3.10) for $K = 2$.

$$
\begin{aligned}
- \quad & \Bigg[\log\left(\beta_1 \cdot |h_1 \cdot u_1|^2 + N_0\right) \\
& - [\log(N_0)] \\
& + \log\left(\beta_2 \cdot |h_2 \cdot u_2|^2 + N_0 + \beta_1 \cdot |h_2 \cdot u_1|^2\right) \\
& - \left[\log\left(N_0 + \beta_1^o \cdot |h_2 \cdot u_1|^2\right) + \frac{|h_2 \cdot u_1|^2}{N_0 + \beta_1^o \cdot |h_2 \cdot u_1|^2} \cdot (\beta_1 - \beta_1^o)\right]\Bigg]
\end{aligned}
\tag{3.17}
$$

Equation (3.17) is negative as the optimisation is a minimum. By getting the minimum of the negative equation we are in fact finding the PA which maximises the sumrate of the system.

To test the iterative algorithm PA against a BFS PA for the same NOMA system. In figure 3.8 we can see that the iterative method can start with an all zero PA and quickly iterate to the optimal PA, achieving the maximum sumrate. This shows, for a 2-UE NOMA system, that the iterative algorithm matches the performance of BFS. The difference however is that the iterative method is much less resource intensive, particularly for high precision of PA or for systems with large numbers of UEs.

As the 2-UE case was successful equation (3.10) was adapted for K UEs.

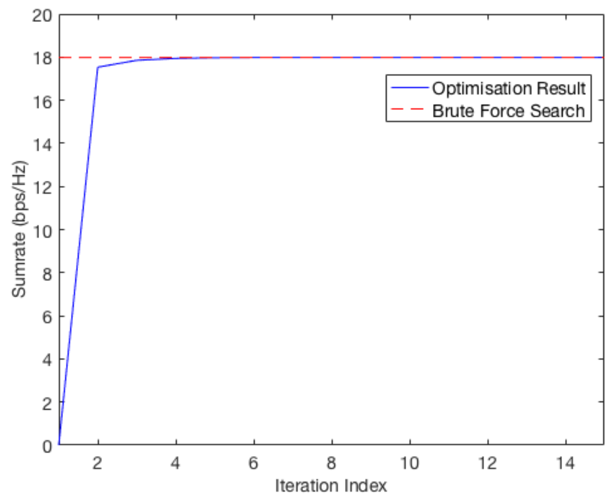

Figure 3.8: Finding 2-UE NOMA Rate by Minimisation or Search

FOA for K UEs

$$
\begin{aligned}
-\sum_{k=1}^{K} \Bigg[& \log\left(\beta_k \left|\mathbf{u}_k \mathbf{h}_k\right|^2 + \sum_{j=1}^{k-1} \beta_j \left|\mathbf{u}_j \mathbf{h}_k\right|^2 + N_0\right) \\
& - \left(\log\left(\sum_{j=1}^{k-1} \beta_j^o \left|\mathbf{u}_j \mathbf{h}_k\right|^2 + N_0\right)\right. \\
& + \frac{\sum_{j=1}^{k-1} \left|\mathbf{u}_j \mathbf{h}_k\right|^2}{\sum_{j=1}^{k-1} \beta_j^o \left|\mathbf{u}_j \mathbf{h}_k\right|^2 + N_0} \\
& \left.\cdot \left(\sum_{j=1}^{k-1} \beta_j - \beta_j^o\right)\right)\Bigg]
\end{aligned}
\tag{3.18}
$$

Equation (3.18) is, like equation (3.17), multiplied by -1 at the start at the optimisation is a minimisation. As the 2-UE equivalent in equation (3.17) was successful, a similar optimisation of equation (3.18) should also find the optimal result for higher values of K. Results of simulations using this iterative method can be seen in figure 3.13.

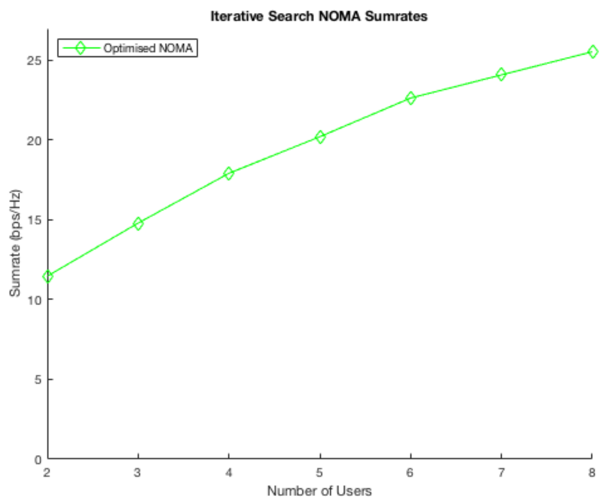

Figure 3.9: Optimised NOMA Results

Comparing figures 3.7 and 3.9, or the same plots in figure 3.13, one can see that the rates achieved using the iterative algorithm match the optimal results found using BFS. The benefit being the dramatic reduction in resources required to find the PA for larger K when using the iterative method.

Though the theoretical sumrates demonstrated in figures 3.7 and 3.9 are impressive with multiple UEs these rates may be worse in practice. The main issues come with the complexity of the receivers in such a NOMA system. If there is an error during SIC error propagation will lead to a lot of resources spent decodign messages of other UEs to find the message was decoded erroneously.

Similarly, even if SIC is carried out without errors the time required to decode many UEs messges would lower the actual throughput of any device, even though the theoretical throughput is high.

Due to the potential issues with larger NOMA systems other NOMA schemes are considered in the rest of this section. These schemes have achieve lower sumrates as the number of UEs increases but should be less susceptible to the issues, outlined above and elsewhere, that arise in larger NOMA systems.

Hybrid NOMA

As is discussed in section 2.4.1 H-NOMA blends traditional MA techniques with NOMA to reduce the complexity required to perform SIC. Here H-NOMA is used such that each orthogonal resource is accessed by no more than 2 UEs. The number of resources groups, M, required can be described as a function of the number of UEs. This is shown in equation (3.19).

$$M(K) = \lfloor K \div 2 \rfloor + K \bmod 2 \tag{3.19}$$

For this implementation of H-NOMA the resources are divided evenly between all M groups. The UEs are grouped based on their channel ranking. As was discussed in section 3.3.1, the strongest un-grouped UE is always paired with the weakest un-grouped UE, as determined by the norm of their channel vectors captured as CSI.

Due to the success of the iterative method it is used to determine the PA of each group in instead of using BFS. As each group has full access to all resources, the 2-UE FOA described in equation (3.17) is used.

The results of simulations with the described H-NOMA system can be seen in figure 3.10.

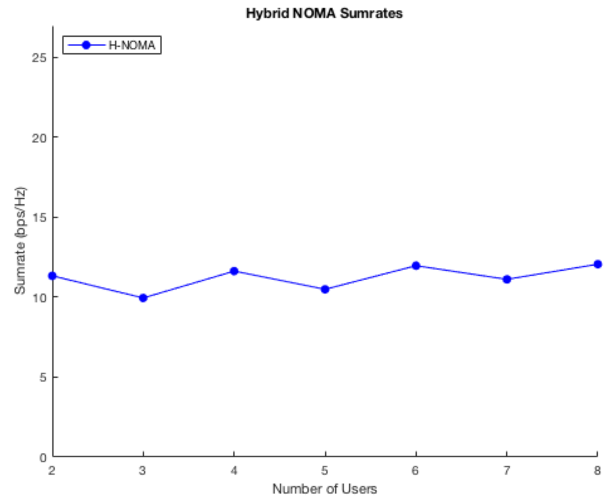

Figure 3.10: H-NOMA Results

Figure 3.10 shows that the sumrate increases within the set of even numbered UEs, where all groups have 2 UEs, and that the sumrate increases within the set of odd numbered UEs, where one group has 1 UE. However, for systems where there is a group with one UE the sumrate is lower than that of a system with one UE less, where all groups are full.

The sumrate for the system is the average sumrate achieved across all resource groups. This would suggest that sumrate should remain relatively consistent as UEs are added to the system, but it was established earlier that NOMA achieves better sumrates with higher numbers of UEs per resource. This explains the decline in sumrate for systems where a resource is occupied by only one UE. Single UE systems bring down the average as they are not taking advantage of the resources to the same extent.

Hybrid NOMA with Proportional Fairness

To combat the underutilisation of resources seen in H-NOMA systems with PF were investigated. Scheduling is the only difference between these approaches to H-NOMA. Rather than splitting the available resources evenly, as with H-NOMA above, in a system using H-NOMA with PF the percentage of resources available to each group corresponds to the relative strength of each resource group. Group strength can be taken as the inverse of the cost of any one group gaining access to the medium, which correlates to the norm of the channel vectors for UEs within a resource group. This can be described by $w_i = \frac{1}{c_i}$ where the weight w_i is equal to the inverse of the cost c_i of letting group i gain access.

The norm of the strongest UE in a group was used as the weight that dictates the proportion of the resource they had access to, as the channel norm already has an inverse relationship with cost. The strongest UE in a group was used as to use the sum of the channel norms would give more weight to groups where the respective UEs had similar channel strengths. Giving preference to these groups is not desirable as they tend to perform worse than groups with greater differences in channel norm. The sum of all weights was normalised such that the resource was fully utilised.

Figure 3.11 shows results from simulations with the described PF H-NOMA system.

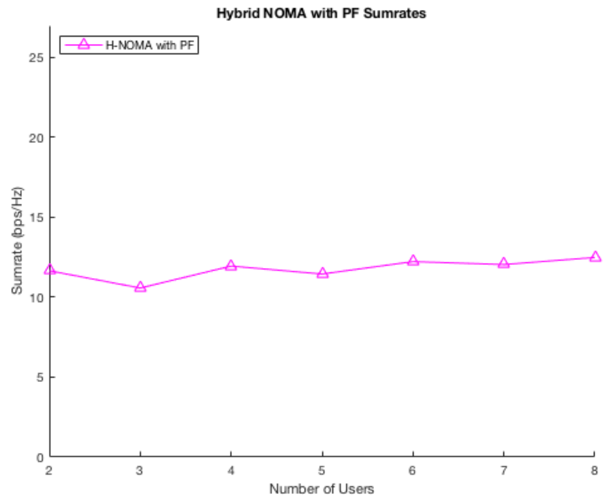

Figure 3.11: H-NOMA with PF Results

By scheduling the UEs with PF there should be a reduction in the sumrate drop caused single UE groups as well as in the sumrate drop caused by generally weaker groups. Ultimately, where H-NOMA saw little benefit to sumrate by adding more UE groups H-NOMA with PF should achieve a slight increase in sumrate when using larger numbers of UEs. It can be seen comparing figures 3.10 and 3.11, or comparing the relevant series in figure 3.13, that PF H-NOMA does achieve better results than H-NOMA and that for greater numbers of UEs the effect of underutilised groups is largely mitigated.

NOMA within Beamforming Beams

NOMA within Beamforming Beams (BF-NOMA), similar to H-NOMA, aims to circumvent the issues with large numbers of UEs in a NOMA system, This is done, as the name of this section suggests, by grouping UEs and targeting them within BF beams then treating each beam as it's own NOMA system. Groups are formed of no more than 2 UEs, so equation (3.19) also describes the number of groups here.

Unlike in H-NOMA groups are not determined by channel strength but rather by the correlation between channels. UEs are first sorted by the norm of their channel vector, then the strongest available channel is cross-correlated with the channels of the remaining UEs and is grouped with the most correlated UE. This is repeated for all UEs.

By grouping UEs with higher channel cross-correlation it is easier to target those UEs with just one beam. However, since the stronger UE is the primary target of the beam the secondary UE will likely achieve a lower throughput. Using one beam to communicate with a pair of UEs allows the BS to treat each beam as its own NOMA system, and therefore simplify SIC for all UEs when compared to a normal NOMA wit BF.

Two approaches to BF-NOMA were considered, both using the iterative method above:

- Arbitrary PA
- Constrained PA

The arbitrary PA approach allows the iterative method to optimise the PA for all UEs entirely arbitrarily. The constrained PA approach divides the available transmission power evenly between all resource groups, or beams. Power is then allocated, using the iterative method, to the UEs in each beam based on the power allotted. Simulations showed the this worked better than arbitrary approach. Arbitrary PA should yield superior results with a BFS but the aim of this investigation was to avoid such a means of PA.

The results of simulations with the described BF-NOMA system can be seen in figure 3.12.

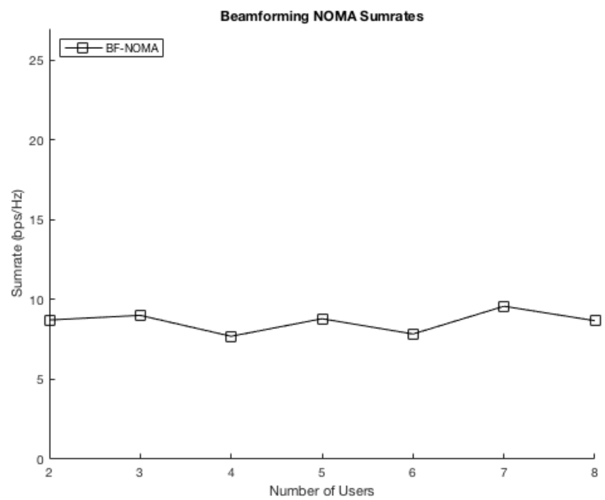

Figure 3.12: BF-NOMA Results

The results shown in figure 3.12 show a weaker, and almost inverted, pattern than that seen in the previous H-NOMA results. In fact, the 2-UE BF-NOMA system is the only one that fails to meet an average of $\sim$11.5 bps/Hz, which can be attributed to one UE, per group, always having a less targeted beam. The inter-UE interference, and the way PA was performed, hindered the sumrates across the board. One can see that for odd numbers of UEs the results are generally superior. This can be explained by beams with only one UE experiencing less contention and interference. Groups with with reduced interference would increase the sumrate overall, which contrasts with single UE groups decreasing sumrate in H-NOMA systems.

3.3.5 Graphical Comparison

By examining the results from the NOMA schemes explored in section 3.3.4 conclusions can be drawn about the effectiveness and efficiency of each relative to competing schemes. Figure 3.13 shows a comparison of those results. A tabular comparison of those results can be found in table A.1.

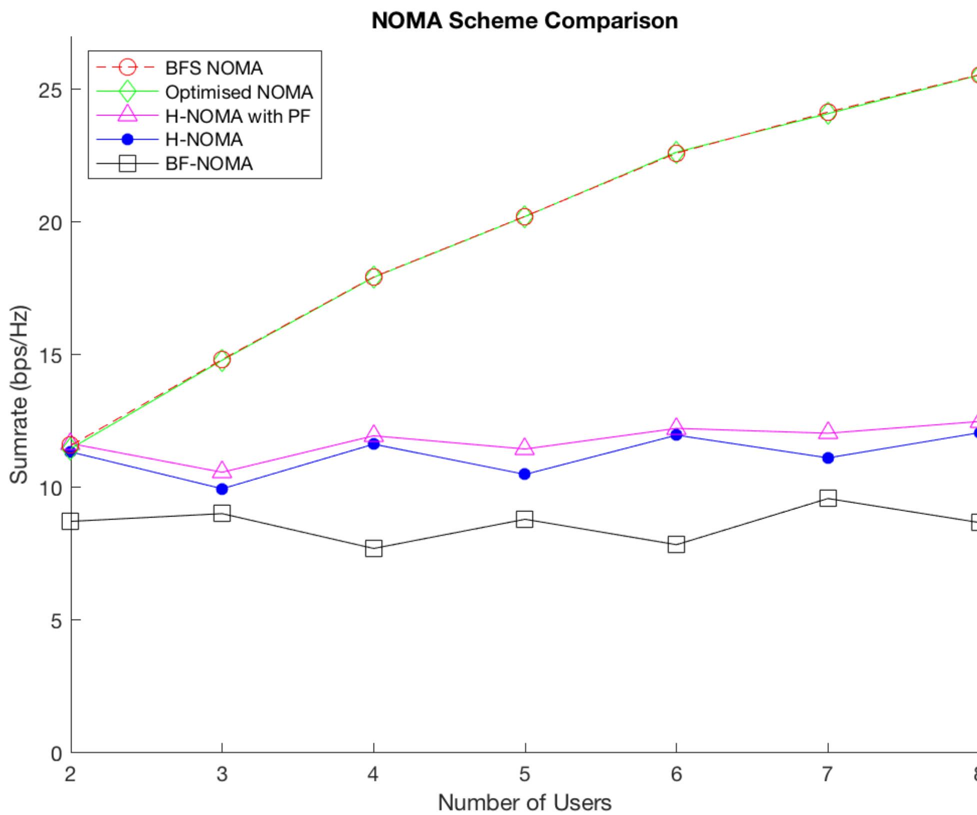

Figure 3.13: NOMA Scheme Comparison

From figure 3.13 it can be seen that the best sumrates were achieved by the BFS method of PA and that the iterative method matched it. Of course, the iterative method achieved matching results in a fraction of the time taken by the BFS, making it a superior method of PA. Though these schemes achieved high throughputs in simulations, the effects of potential SIC errors make other schemes more appealing for larger groups of UEs.

It is clear that both H-NOMA with PF and H-NOMA are the UPPA schemes which achieve the next best results, with the PF variant showing better results. PF especially showed better results than round robin scheduling in systems with odd numbers of UEs. H-NOMA with PF was able to perform better by compensating for systems which were yielding lower throughputs. Both H-NOMA schemes are underutilising the available resources, by design to reduce strain on SIC.

BF-NOMA was considered as a means of striking a balance between the simplicity of H-NOMA and the throughput of full NOMA. Completely arbitrary PA yielded very poor results, as the optimisation failed to find the global minimum but rather always found local minima which yielded low sumrates. Constraining the PA for the system did improve the throughput but it did not outperform H-NOMA as desired. This is a result of two significant disadvantages; poorly correlated UE channels, and inter-beam interference. These obstacles to BF-NOMA proved too great for it to achieve sumrates comparable to any of the other schemes.

Chapter 4

Discussion and Conclusions

This chapter aims to discuss, and draw conclusions from, the results seen in chapter 3, in the context of the methods documented in that chapter. This includes the selection of a channel model, choosing an appropriate BF algorithm, and the evaluation of different NOMA schemes and their merits. These aspects are all examined with respect to their suitability for NOMA with BF in mmWave spectrum.

4.1 Finding a Suitable Channel Model

A suitable channel model, for our purposes, was one which was accurate for mmWave spectrum and erred on the side of pessimism when calculating the PL seen across the channel. A good foundation as a mmWave channel is important as the use of mmWave spectrum is a core tenant of this thesis and as such was of great importance. With the aim of finding a channel model that would be indicative of real mmWave channels it was important to choose a channel which gave harsher PL results rather than more encouraging results. Using such a channel would allow for more confidence in the effectiveness of NOMA systems as the systems would be tested in worse case scenarios.

The parameters of the channel were to find a channel indicative of one over mmWave 28 GHz, a likely spectrum allocation for FRA, and NLOS, representative of the modal LOS in current networks.

4.1.1 Friis' Transmission Equation

Friis' Transmission Equation for PL was assumed, and was later shown, to be too simplistic for a mmWave channel model. However, it made for an interesting contrast to two more likely channel model candidates as the both PLE and Samsung's model were adaptations to this simplistic PL equation. Friis' Equation was not under proper consideration but was merely used as a benchmark for a known reference.

4.1.2 Path Loss Exponent

In contrast with Friis' PL equation, the addition of a parameter β to PLE equation leads to more realistic results. Since the β term can be manipulated to fit the PLE results it can theoretically be tuned to be quite accurate. With this in mind, when using a value of 3.4, which is typically used for 28 GHz NLOS systems, expectations were that the results should be promisingly realistic.

It was later seen that the results from the PLE channel model were the closest to the NYU model that was used.

4.1.3 NYU Empirical Model

The NYU model, as it was empirical and modelled off of measurements taken in New York City, seemed most likely to be a strong model going into the simulations done in section 3.1. NYU's model bares resemblance to the PLE equation, with β also encompassing the pre-calculated constants based on the frequency used. The addition of an α term and fitting the β parameter to the measured results gave rise to a better founded channel model than those examined earlier in the chapter.

4.1.4 Comparing Models

Figure 3.1 shows a comparison of the models discussed above. It is clear from the figure that the results were close to what was expected.

The Samsung model, based upon the reference Friis' Transmission Equation for PL, seemed too optimistic by $\sim$10 dB. As this short coming is consistent for both the CCU and the CEU it could perhaps be adapted to give better results for mmWave spectrum. However, as the aim was not to propose a channel model but rather to find a suitable one it was discarded.

The PLE equation for PL was clearly less harsh on the CCU than the CEU in a way that seemed plausible. However, the results seemed too optimistic to make for good testing, particularly at the CCU. Non-linear attenuation over the channel, shown in the PLE case as compared to the Friis' and Samsung cases, could be expected from a mmWave channel due to the extra interactions of mmWaves with the atmosphere. This shows that the PLE channel model did have promise with the values selected.

The NYU model gave results which seem the best justified by their approach as well as being the most pessimistic in their indication of received signal strength. Pessimistic results can make for a good test scenario, as the results can be more interesting than the best case results. The fact that these results are also consistent with other channel models and seem well founded in the source material makes the NYU channel model a strong basis for the examinations of NOMA which followed.

4.2 Basic NOMA Simulations

Simulating NOMA using purely PA, and no BF, was important for benchmarking the success of NOMA systems with BF later. As the systems were performing PA via BFS it was only feasible to simulate small numbers of UEs, so 2-UE cells were simulated.

4.2.1 System Model

The channel for UEs was based on the NYU model discussed earlier. Small scale fading was factored into the NYU predicted PL to add further variation to the channels tested.

PL is a function of distance. The distances used fell within the range of 50 m to 250 m for all UEs in the attached to the BS.

The optimal PA was found using BFS. BFS is inefficient and restricted the scope of these simulations to only a small number of UEs, for which the inefficiency was still acceptable.

4.2.2 Simulation Results

In these simulations NOMA greatly favoured the CCU in the majority, to the extent that the CEU was almost always excluded if the aim was to maximise the system throughput. This result was discouraging as it implied that sumrate was higher when using OMA for MA instead of NOMA.

Of course, improvements were seen to sumrates once NOMA with BF was considered.

4.3 Beamforming NOMA

Considering NOMA with BF became necessary once it was apparent that the results from basic NOMA were not sufficient, and were failing to improve sumrates. The problem was broken in two, considering BF direction and PA separately. In sum, section 3.3 showed that the using NOMA with BF algorithms gave a good boost to sumrates and spectral efficiency.

Random BF precoders showed that BF was indeed a viable way to improve earlier results, though it was not practicable due to the nature of the BFS used.

Later examination of BF algorithms showed that MRT had an advantage over the results seen from ZF. This investigation lead MRT to be adopted as a BF precoder for the rest of the work conducted in this thesis.

Simulations testing various PA and UPPA schemes showed that the iterative method of PA had optimal performance with great efficiency. While full NOMA systems performed well in simulation, H-NOMA with PF is potentially a better alternative for systems with larger numbers of UEs due to issues likely to occur at receivers.

4.3.1 System Model

The system model for NOMA with BF differed from the basic NOMA model primarily through the addition of extra antennas at the BS and the considerations which come with that. The main considerations being how the channel is now represented as a vector and PA can be done with BF to direct power towards a UE.

The introduction of BF changes the problem of maximising sumrate from purely considering PA or UPPA, as is the case in basic NOMA, to one of targeting beams and PA or UPPA.

4.3.2 Random Beamforming

Random BF was used to determine the feasibility of NOMA with BF over basic NOMA. By generating random beams, using brute force, it means that the viability of BF can be assessed without tying the results to a specific BF algorithm.

Assessing the success of BF in this way gave strong indication that NOMA with BF would yield greater sumrates than were seen in earlier simulations. Unlike in section 3.2, in section 3.3 the sumrates were maximised by including more UEs and by leveraging NOMA to improve the spectral efficiency.

This result was seen in simulations with both two and three UEs connected to a BS. Demand on computational resources from using a BFS for both PA and BF precoders ruled out the possibility of simulations with more UEs. However, from early the results it could be extrapolated that BF with NOMA should also benefit systems with more

UEs.

The inefficient use of resources required to generate and test random BF precoders also motivated the use of BF algorithms to more efficiently and effectively produce good beamformers. Random BF proved that the use of such algorithms should be capable of generating effective beams and improving the sumrate of NOMA systems.

4.3.3 Beamforming Algorithms

As the problem of effective PA for NOMA had not been tackled yet BFS was still used to find the optimal PA for each system. Once again, using BFS restricted the number of UEs to be small. In this case, simulations were performed with two UEs.

Both BF algorithms used generated a BF precoder, which would determine only the of the beams. The algorithms considered were MRT and ZF. Use of these algorithms is widespread and both determine the BF precoder by performing mathematical operations based on the CSI for the set of UEs attached to the BS.

ZF promised to pose lower inter-UE interference, which may boost sumrate by giving the SINR of each UE a smaller denominator. This property of ZF is what gives it its name. The ZF algorithm prioritises lowering interference between UEs over improving the throughput of the UE.

MRT, in contrast with this philosophy, maximises the transmission of each UE in their direction, without consideration of the effects of the beam on other UEs. This property of MRT maximises the numerator of each UE's SINR. This should also do well to boost the sumrate of the system as each UE should contribute more to the sumrate without being overly hindered by inter-UE interference.

Examining figure 3.6 and table 3.1 it can be seen that, on average, both BF algorithms achieved almost exactly the same maximum sumrate, though MRT produced better sumrates at all other values. Though both algorithms seem equally well suited to NOMA systems, MRT was chosen for use for the remainder of simulations due to its slight advantage.

4.3.4 User Pairing and Power Allocation for Beamforming NOMA

Different UPPA schemes were examined to investigate the best means of leveraging NOMA with BF.

Of course, methods for using full NOMA were considered, as well as processes which could perform it efficiently. Full NOMA with an iterative method of PA proved most successful at this.

Other NOMA schemes were also evaluated as alternatives, under the assumption that NOMA may become less effective with large numbers of UEs. Amongst these alternate schemes H-NOMA with PF yielded the highest sumrates.

Brute Force Search

Using BFS for PA in NOMA yields the optimal solution to maximise sumrate. However, the process is too resource intensive for practical networks, as the CSI which the PA was based on is likely to change by the time the BFS completes.

For large numbers of UEs the set of possible PAs is so large that generating the set of possible combinations takes a lot of time. This is before computing the theoretical throughput for each subset.

The computations required to perform an exhaustive search grows exponentially as the number of UEs increases. The number of PA combinations required for an n-UE NOMA renders this approach unusable.

Given the issues with using BFS other methods of PA must be considered as it is not viable.

Iterative Algorithm

To improve on the efficiency of the BFS, while maintaining its effectiveness, an iterative algorithm was employed. As the sumrate is a non-convex function, an FOA of the sumrate was iterated upon. By using an FOA the iterative algorithm is capable of finding an equally optimal solution, compared to the BFS, with greatly improved use of computational resources.

As was shown in figure 3.13, this iterative method of PA for NOMA systems yielded results which matched those found with the BFS. Such results make this the favourable method of PA for NOMA systems.

The drawbacks seen with larger numbers of UEs in NOMA systems — receiver complexity and SIC error propagation — may reduce actual throughput and make NOMA less appealing for those systems. The method of PA, of course, is still highly effective regardless of other issues seen in these systems.

Hybrid NOMA

H-NOMA is a method of UPPA which is widely discussed in the literature as a means of combating the issues outlined above. Pairing UEs with the greatest difference in channel norms, determined by measured CSI, guarantees the best sumrate for the system as a whole. Pairing UEs into resource groups reduces the complexity needed in receivers and throughput issues resulting from them, but limits the maximum sumrate.

As UEs are added to the H-NOMA system throughput does not increase in the way that was seen in full NOMA. Instead the throughput oscillates and varies for odd and even numbers of UEs, with even numbers achieving greater results due to better utilisation of the resources available.

Hybrid NOMA with Proportional Fairness

Using PF scheduling, instead of round robin scheduling, with H-NOMA was a way to reduce the impact of underutilised resource groups on sumrate. Improving the sumrate of H-NOMA is important since the maximum sumrate is so low in comparison to a full NOMA system.

PF as an alternative method of scheduling achieved this goal. Not only was PF successful at improving the sumrates for systems which had only one UE in a resource group, using this method of scheduling also helped increase the sumrates of systems with fully paired groups when compared to H-NOMA. This can be seen in figure 3.13, where the sumrates climb slightly higher as UEs are added.

NOMA within Beamforming Beams

BF-NOMA was conceived of as a method of improving upon the limitations to throughput caused by H-NOMA's approach to splitting resources. It can be seen, when contrasting full NOMA with H-NOMA, that using power as the resource which is shared among UEs has the least detrimental impact on throughput. Taking that as inspiration, BF-NOMA aimed to merge the concept of resource groups (taken from H-NOMA) with the concept of using power as the resource which is being shared (taken from NOMA).

Using BF-NOMA has some clear advantages and disadvantages when compared to H-NOMA. By only splitting PA it bears the closest resemblance to the NOMA systems described when considering BFS and the iterative method, both of which achieved optimal results. The results from those optimal simulation sets suggests that power is the best resource to split, which is the resource being split in BF-NOMA.

However, a considerable drawback of BF-NOMA is inter-UE interference which is caused by other resource groups, or beams. These beams are outside the scope of SIC and reduce sumrate. The impetus to investigate BF-NOMA was to lessen the potential reduction in throughput caused by poor SIC, while BF-NOMA's avoidance of SIC is its downfall.

4.4 Conclusion

The literature surrounding NOMA shows that important areas for improvement include optimising UPPA, and reducing receiver complexity. When also considering the mmWave spectrum it can be seen that there is not an agreed channel model for use in examining mobile communications.

Strengths of this thesis include how the work based is based upon a well founded channel model and the examination of BF algorithms which lend themselves to use in

NOMA systems. Evaluating UPPA schemes which leverage NOMA to improve spectral efficiency, with consideration given to receiver complexity, is another strength as these issues are highlighted in existing literature as problems facing NOMA.

Figure 3.13, and table A.1, show that results confirming the point made in section 4.3.4.

The results from BFS and the iterative method of PA clearly maximise theoretical sumrates for those systems, with the iterative approach being superior in practice. Using an iterative algorithm for PA is certainly the best for a full NOMA system. The iterative method of PA is very successful in solving the problem it aims to address. Achieving equally successful results 900× faster than using BFS makes NOMA feasible in practice. Unlocking this potential is the greatest contribution of this thesis to the literature.

H-NOMA with PF offers the best performance for maximising sumrate while simplifying the SIC process amongst the remaining NOMA schemes. BF-NOMA failed to achieve the same rates all other offerings in a 2-UE case, due to poor correlation between channels. H-NOMA performed relatively well but was subject to significant losses in sumrate when a resource group served only one UE.

BF-NOMA may be capable of matching the benefits of H-NOMA, and reducing receiver complexity, while overcoming its short comings, the limit to sumrate seen earlier. However, this was not achieved in the testing and simulations conducted as part of this thesis. Based on the results in this thesis alone, BF-NOMA is not as good a solution to MA as NOMA or H-NOMA.

H-NOMA with PF is another strong contribution offered by this thesis. Alternatives to full NOMA systems will be needed given the complexity of those systems and H-NOMA is a good alternative. By taking advantage of existing, well developed, and wide spread MA technologies as well as NOMA it improves spectral efficiency without the increase in overhead seen in full NOMA. While the theoretical throughputs of full NOMA systems are high they may be much lower in practice. A reduction in throughput could be seen by error propagation or simply the time taken by CCUs to decode their messages after decoding the messages of all other CEU.

NOMA with BF in mmWave spectrum is very promising. The sumrates achievable by NOMA and H-NOMA show that the spectral efficiency of this MA technology is superior to OMA systems. Improved MA is greatly needed to meet the ever-increasing demand for more connected devices. As we move towards using mmWave spectrum, NOMA with BF will enable that transition and the devices that come with it.

Chapter 5

Impact of the Research

The impact of this research may be seen in FRA. An example of which would be 5G networks. The proposed methods of improving spectral efficiency, through improved MA, would allow an increase to the number of connected devices in mobile networks.

In my opinion, NOMA will give rise to a more densely connected society, which has the potential to be life enriching. A network with more connected devices, and better throughputs, would further the spread of ideas and allow for growth in areas such as the Internet of Things. Exactly what will be done with the increased capacity for new devices is, as yet, unclear. In the rest of this chapter, we will explore areas which are already on the cusp of breakthrough, but require improved connectivity.

Using more efficient MA to enable more Internet of Things devices has great potential to changing how we interact with the world. Smart systems, integrated with our homes and cities, will improve automation and reduce friction in our everyday lives. These technologies already exists to an extent so we can see the potential for further development. As these systems develop they will allow people to effortlessly take greater, and more direct, control of their living environment. When the buildings we live and work in become smarter the technologies will smoothly provide a more comfortable living and working space while being less impactful on resources such as electricity and heat. This will also have a positive benefit on the environment and climate.

We are already in an age of wearable devices. By using NOMA variants to increase the capacity for connectivity, future wearable devices will be able interact more continuously and deeply with the world around them. Growing the capacity of networks to allow these connections will allow the seamless transfer of medical data between people and health care services. This opens up the possibility for consumers to be better informed and more closely monitored in relation to their health. In an ageing population this may to help maintain the well being of the users of these wearable devices, while taking pressure off a busy health care system.

FRA will increase throughputs generally, but the effects will be most profound in rural communities. Improved connectivity in rural areas will have positive implications for many aspects of life. Infrastructure for traditional networks, such as broadband, are cost inhibitive, whereas Radio Access Networks (RAN) have lower installation costs. Better data rates could be achieved with RAN, without the need to upgrade the existing infrastructure. Bringing improved data networks to rural communities will empower them and lessen the strain on cities. This may be realised by enabling people in those areas to work or study remotely.

Chapter 6

Suggestions for Future Work

This chapter will discuss areas directly related to the research carried out in this thesis which could benefit from further research. Suggestions for the aims of further research will also be given.

6.1 NOMA within Beamforming Beams

BF-NOMA was considered as an alternative to H-NOMA in attempts to reduce receiver complexity required by full NOMA. Though theoretically promising, it was the worst performing NOMA scheme considered in section 3.3.4. BF-NOMA's shortcomings in simulations, given the theoretical potential for success, make it the topic most in need of further research.

A fundamental issue with BF-NOMA is most apparent in the 2-UE case. In 2-UE systems the use of one beam to target two UEs often leads to poor results for the weaker CEU. This is a direct result of low channel correlation reducing the strength of the received signal at one UE. This, of course, lowers throughput. An area that requires further research is a BF algorithm which effectively targets two UEs simultaneously, potentially determining the degree of channel correlation sufficient to do so.

Further effort still should be invested in to optimising PA for BF-NOMA. While constrained PA yielded the best results in simulations conducted as part of this research, it makes intuitive sense that this method of PA would not yield the optimal result. If it was, arbitrary PA optimisations should lead to the same results.

When applying the iterative method, which was very successful for full NOMA and H-NOMA, to BF-NOMA the results were very poor. The success of constrained PA for BF-NOMA, over completely arbitrary PA, implies that the FOA seen in equation (3.18) does not sufficiently convexify the sumrate of BF-NOMA.

Research should be undertaken to find an optimal method of PA for BF-NOMA, which does not require BFS. As BF-NOMA lessens the complexity of full NOMA, and since better PA may offer substantially improved sumrates to H-NOMA, it may be the best alternative to full NOMA if successful.

6.2 Scheduling Algorithms

The use of PF scheduling improved upon round robin scheduling in the case of H-NOMA. Using PF made this alternative NOMA scheme more useful and improved upon some of H-NOMA's greatest issues.

Though PF was used in this case the use of scheduling algorithms in other NOMA schemes, or even of other scheduling algorithms with H-NOMA, were not considered.

Failing to examine alternative scheduling algorithms, or the use of these algorithms in other contexts, requires an investigation into their potential benefits in the future.

A means of evaluating other scheduling algorithms could, of course, be the maximisation of the sumrate of NOMA systems. Another possibility would be to evaluate the success of these algorithms in their some sort of fairness based sumrate or a variation of sumrate which favours one class of UE.

6.3 Beamforming Algorithms

As was mentioned in section 6.1, future research could be conducted in search of improved BF algorithms for NOMA. There is also potential for alternate algorithms to improve BF in other schemes, though BF-NOMA is the most glaring example.

The primary issue, with regard to BF algorithms, in the BF-NOMA context is the pairing of UEs within a beam. The aim, therefore, of such a BF precoder may be to optimise sumrate by giving consideration to the correlation of the channels for the targeted UEs. The algorithm should choose a precoder which optimises sumrate within the beam or shows some degree of fairness between UEs in that beam, based on factors such as channel norm.

Other research in this area could consider other algorithms than ZF and MRT in the context of NOMA systems. Investigating only two BF algorithms could be seen as quite narrow. It could also be seen if different algorithms lend themselves better to certain NOMA schemes, as the MRT was chosen solely from results of a 2-UE full NOMA system.

Bibliography

[1] Z. Ding, X. Lei, G. K. Karagiannidis, R. Schober, J. Yuan, and V. K. Bhargava, "A survey on non-orthogonal multiple access for 5g networks: Research challenges and future trends," *IEEE Journal on Selected Areas in Communications*, vol. 35, pp. 2181–2195, Oct 2017.

[2] Y. Saito, Y. Kishiyama, A. Benjebbour, T. Nakamura, A. Li, and K. Higuchi, "Non-orthogonal multiple access (NOMA) for cellular future radio access," in *2013 IEEE 77th Vehicular Technology Conference (VTC Spring)*, pp. 1–5, June 2013.

[3] M. B. Shahab and S. Y. Shin, "User pairing and power allocation for non-orthogonal multiple access: Capacity maximization under data reliability constraints," *Physical Communication*, vol. 30, pp. 132 – 144, 2018.

[4] A. Wiesel, Y. C. Eldar, and S. Shamai, "Zero-forcing precoding and generalized inverses," *IEEE Transactions on Signal Processing*, vol. 56, pp. 4409–4418, Sep. 2008.

[5] S. Hu and F. Rusek, "A generalized zero-forcing precoder for multiple antenna gaussian broadcast channels," in *2017 IEEE International Symposium on Inform-*

ation Theory (ISIT), pp. 556–560, June 2017.

[6] E. Björnson, M. Bengtsson, and B. Ottersten, "Optimal multiuser transmit beamforming: A difficult problem with a simple solution structure [lecture notes]," *IEEE Signal Processing Magazine*, vol. 31, pp. 142–148, July 2014.

[7] G. C. Alexandropoulos and M. Kountouris, "Maximal ratio transmission in wireless poisson networks under spatially correlated fading channels," *CoRR*, vol. abs/1508.06440, 2015.

[8] Z. Ding, P. Fan, and H. V. Poor, "Impact of user pairing on 5g nonorthogonal multiple-access downlink transmissions," *IEEE Transactions on Vehicular Technology*, vol. 65, pp. 6010–6023, Aug 2016.

[9] A. Li, A. Harada, and H. Kayama, "A novel low computational complexity power assignment method for non-orthogonal multiple access systems," *IEICE Transactions*, vol. 97-A, pp. 57–68, 2014.

[10] T. Yazaki and Y. Sanada, "Effect of joint detection and decoding in non-orthogonal multiple access," in *2014 International Symposium on Intelligent Signal Processing and Communication Systems (ISPACS)*, pp. 245–250, Dec 2014.

[11] S. M. R. Islam, "Noma in 5g systems: Exciting possibilities for enhancing spectral efficiency," *IEEE Future Networks*, Jun 2017. Accessed:2018-09-25.

[12] S. M. R. Islam, N. Avazov, O. A. Dobre, and K. Kwak, "Power-domain non-orthogonal multiple access (noma) in 5g systems: Potentials and challenges," *IEEE Communications Surveys Tutorials*, vol. 19, pp. 721–742, Secondquarter 2017.

[13] F. Khan and J. Pi, "Millimeter-wave mobile broadband: Unleashing 3-300ghz spectrum." https://eclass.duth.gr/modules/document/file.php/TMA191/Farooq%20Khan-RF-Systems-Mobile%20Broadband-unleasing-t1.pdf, Mar 2011. Accessed:2019-01-16.

[14] S. Sun, G. R. MacCartney, and T. S. Rappaport, "Millimeter-wave distance-dependent large-scale propagation measurements and path loss models for outdoor and indoor 5g systems," in *2016 10th European Conference on Antennas and Propagation (EuCAP)*, pp. 1–5, April 2016.

[15] M. K. Samimi and T. S. Rappaport, "3-d millimeter-wave statistical channel model for 5g wireless system design," *IEEE Transactions on Microwave Theory and Techniques*, vol. 64, pp. 2207–2225, July 2016.

[16] J. Lee, J. Choi, J. Lee, and S. Kim, "28 ghz millimeter-wave channel models in urban microcell environment using three-dimensional ray tracing," *IEEE Antennas and Wireless Propagation Letters*, vol. 17, pp. 426–429, March 2018.

[17] M. R. Akdeniz, Y. Liu, M. K. Samimi, S. Sun, S. Rangan, T. S. Rappaport, and E. Erkip, "Millimeter wave channel modeling and cellular capacity evaluation," *IEEE Journal on Selected Areas in Communications*, vol. 32, pp. 1164–1179, June 2014.

[18] T. Nguyen, "Qoro - small cell networks and the evolution of 5g." https://www.qorvo.com/design-hub/blog/

`small-cell-networks-and-the-evolution-of-5g`, May 2017. Accessed:2019-01-17.

Appendix D: Hazard Identification / Risk Analysis

SCHOOL OF ELECTRICAL & ELECTRONIC ENGINEERING

ME ELECTRICAL ENERGY ENGINEERING or ME ELECTRONIC & COMPUTER ENGINEERING

Please complete and return **two copies** of this form to the School of Electrical & Electronic Engineering Office, Room 226 by **4 pm on Friday 28th September 2018** (c/o Damian Flynn or Mark Flanagan). One copy will be retained by the School. The other copy is retained by you as proof that your completed form has been received. At the end of the project you should include a copy of this form in your final report.

Student Name:	Cian Dowd	Signature
Student Number:	14302446	
Supervisor:	Nam Tran	Signature
Project Title:	Beamforming for Millimeter-wave NOMA	
Programme:	ME Electrical or Electronic & Computer Engineering	

Identify any potential safety hazards for your project, e.g. dangerous voltages, rotating machinery, radiation, soldering fumes, sitting in front of a computer for prolonged periods

Tendonitis in arms aggrevated by typing and writing.
Stiff neck/back from working at a computer for prolonged times.

Indicate how all identified safety hazards will be managed to provide a safe working environment

Ergonomic pens
Ergonomic keyboard and mouse
Laptop stand
Regular breaks from work
Stretches

Office Use Only

Date and Time Received: UCD School of Electrical and Electronic Engineering 28 SEP 2018 [School Stamp]	**Received by:**
	Document Tracking
	Lecturer:

Appendices

Appendix A

Tabular Comparison of NOMA Schemes

Table A.1: NOMA Scheme Comparison

Number of UEs	2	3	4	5	6	7	8
BFS NOMA	11.6	14.8	17.9	20.2	22.6	24.1	25.6
Optimised NOMA	11.5	14.8	17.9	20.2	22.6	24.1	25.5
H-NOMA with PF	11.7	10.6	12.0	11.5	12.2	12.0	12.5
H-NOMA	11.3	10.0	11.6	10.5	12.0	11.1	12.1
BF-NOMA	8.7	9.0	7.7	8.8	7.8	9.6	8.7